Ternary nucleation of inorganic acids, ammonia, and water

I. Napari,[a] M. Kulmala, and H. Vehkamäki
Department of Physical Sciences, P.O. Box 64, 00014 University of Helsinki, Finland

(Received 3 June 2002; accepted 14 August 2002)

Homogeneous ternary nucleation rates of water, ammonia (NH_3), and inorganic acids are calculated from classical nucleation theory at various combinations of temperature and ambient vapor concentrations. Mixtures with sulfuric acid (H_2SO_4), nitric acid (HNO_3), hydrochloric acid (HCl), and methane sulfonic acid (CH_3SO_3H or MSA) are considered. The results are compared to assess the relative importance of different nucleation routes. Vapors with an acid and an alkaline (ammonia) component are shown to nucleate more readily than vapors having two acid species. Much lower concentrations of H_2SO_4 than HNO_3 or HCl are required to reach the same nucleation rate at similar vapor concentrations of H_2O and NH_3. Nucleation rates in H_2O–H_2SO_4–HNO_3 and H_2O–H_2SO_4–MSA vapors are close to the limit of H_2O–H_2SO_4 nucleation, even at high concentrations of MSA and HNO_3. The results suggest that H_2O–H_2SO_4–NH_3 nucleation is the foremost ternary nucleation route in the atmosphere. © *2002 American Institute of Physics.*
[DOI: 10.1063/1.1511722]

I. INTRODUCTION

Homogeneous nucleation of water and sulfuric acid (H_2SO_4) has been long considered as the primary pathway for the production of new particles in the atmosphere. However, growing evidence from field measurements[1–5] indicates that H_2O–H_2SO_4 nucleation is not able to account for the observed particle formation in many conditions. Recent work[6,7] has shown that ternary nucleation of water, sulfuric acid, and ammonia (NH_3) has the potential of explaining the observations, but, along with enhancement processes for binary nucleation,[8,9] other ternary nucleation routes are still open to critical discussion.

Our purpose in this paper is to study ternary nucleation in aqueous vapor mixtures of ammonia and inorganic acids commonly found in the atmosphere. In addition to the recent studies of H_2O–H_2SO_4–NH_3 system[6,7] earlier theoretical work on ternary nucleation in water–hydrochloric acid (HCl)–ammonia[10] and water–sulfuric acid–methane sulfonic acid (CH_3SO_3H or MSA)[11] vapors has been done during the last decade. All these studies suffer from differences both in the thermodynamic modeling and the treatment of nucleation kinetics. Therefore, a reliable comparison between the above mentioned nucleation routes is not feasible if solely based on published results. Our aim is to make a consistent comparison of nucleation rates between different ternary systems. We will consider vapors containing water, ammonia, and an inorganic acid, or, alternatively, two inorganic acids. The acids are sulfuric acid, nitric acid, hydrochloric acid, and MSA. We do not aim to develop new thermodynamic models; instead, we use existing models from published sources as much as possible and make necessary adjustments to them.

The presented choice of substances allows us to make comparisons from two perspectives. First, we can assess the effect of ammonia on water–acid systems, where the acid is H_2SO_4, HNO_3, or HCl. Second, recalling the importance of sulfuric acid in the atmosphere, we can add a second inorganic acid component (or ammonia) to H_2O–H_2SO_4 vapors. (Unfortunately, we have to omit H_2O–MSA–NH_3 and H_2O–H_2SO_4–HCl systems, because there are no existing thermodynamic models for these systems.) Thus, the systems can be divided into two groups, namely

H_2O–H_2SO_4–NH_3,

H_2O–HNO_3–NH_3,

H_2O–HCI–NH_3,

and

H_2O–H_2SO_4–NH_3,

H_2O–H_2SO_4–HNO_3,

H_2O–H_2SO_4–MSA.

It should be noted that H_2O–H_2SO_4–NH_3 is included in both the groups. However, depending on the group, the nucleation rate is calculated in a slightly different way, as explained later. Because the systems in the first group contain an acid and an alkaline component while in the second group two acid substances are present, we expect considerable differences in the nucleation behavior between the two groups. Most of the comparisons are done at 298.15 K, mainly because the thermodynamics of the mixture containing MSA is applicable only at this temperature.

The theoretical framework is based on classical nucleation theory. Although detailed in our previous paper,[7] we give an outline of the theory in Sec. II. The thermodynamic models are explained in Sec. III. Section IV is devoted to the exposition of our numerical calculations, where each group of systems is considered separately. Because the enhancement of binary H_2O–H_2SO_4 nucleation by ammonia was

[a]Author to whom correspondence should be addressed. Electronic mail: ismo.napari@helsinki.fi

 © 2002 American Institute of Physics

Downloaded 28 Nov 2002 to 128.214.57.32. Redistribution subject to AIP license or copyright, see http://ojps.aip.org/jcpo/jcpcr.jsp

initially predicted from the ability of ammonia to decrease sulfuric acid vapor pressure above a solution surface,[12] we place an additional emphasis on the acid pressures over the ternary solutions. Finally, in Sec. V we present a summary of our results and discuss atmospheric implications.

II. THEORY OF TERNARY NUCLEATION

The Gibbs free energy of formation of an incompressible liquid cluster in an ideal ternary vapor can be written as[13]

$$\Delta G = -kT\sum_{i=1}^{3} n_i \ln\left(\frac{p_i}{p_{s,i}}\right) + 4\pi\sigma r^2, \tag{1}$$

where k is the Boltzmann constant, T is absolute temperature, and the index i enumerates the molecular species. For each species, n_i is the total number of molecules, p_i is the ambient partial pressure of free molecules, and $p_{s,i}$ is the equilibrium vapor pressure above a flat solution surface. The radius of the spherical cluster is r. Surface tension of the droplet is assumed to be the same as that of a flat solution surface at the composition of the nucleus. The number of molecules in the droplet are divided into two parts: $n_i = n_{il} + n_{is}$, where n_{il} gives the numbers of molecules in the uniform liquid phase and n_{is} corrects for the difference between the density profiles of the uniform liquid droplet and the real cluster.

The critical cluster corresponds to the minimum of Gibbs free energy with respect of particle numbers n_i. Minimization of Eq. (1) gives

$$\ln\left(\frac{p_1}{p_{s,1}}\right) v_2 = \ln\left(\frac{p_2}{p_{s,2}}\right) v_1, \tag{2}$$

$$\ln\left(\frac{p_3}{p_{s,3}}\right) v_2 = \ln\left(\frac{p_2}{p_{s,2}}\right) v_3, \tag{3}$$

where v_i is the partial molar volume of component i. These equations are solved numerically for the composition of the critical cluster. The formation energy of the critical cluster ΔG^* is then obtained with the help of the Kelvin equation,

$$r^* = \frac{2\sigma v_i}{kT \ln(p_i/p_{s,i})}, \tag{4}$$

from

$$\Delta G^* = \tfrac{4}{3}\pi r^{*2}\sigma, \tag{5}$$

where r^* is the radius of the critical cluster.

The general formula for the nucleation rate is[14]

$$J = \frac{|\lambda|/\pi}{\sqrt{-\det(\mathbf{D})/\pi}}\rho(\{n_i\}), \tag{6}$$

where $\mathbf{D}$ is a matrix with elements,

$$D_{ij} = \frac{1}{2kT}\left.\frac{\partial^2 \Delta G(\{n_i\})}{\partial n_i\, \partial n_j}\right|_{\{n_i^*\}} \quad (i,j = 1,2,3), \tag{7}$$

and λ is the negative eigenvalue of matrix $\mathbf{KD}$, where $\mathbf{K}$ is the condensation matrix, the elements of which are related to the collision rate of vapor particles with the critical cluster of size $\{n_i^*\}$.[15] As in our previous studies of H_2O–H_2SO_4 and H_2O–H_2SO_4–NH_3 systems,[7,16] the colliding molecules in vapors containing H_2SO_4 are monomers of H_2O, H_2SO_4, and NH_3 as well as hydrates consisting of one acid molecule and up to five water molecules. If the vapor does not contain H_2SO_4, only monomers are considered as colliding particles.

The equilibrium distribution of clusters containing n_i molecules $\rho(\{n_i\})$ is also needed to calculate the nucleation rate from Eq. (6). For H_2O–H_2SO_4–NH_3/HNO_3/HCl systems we use the distribution given by[17]

$$\rho(\{n_i\}) = \rho_2\left(\frac{\rho_1}{\rho_0}\right)^2 K_1K_2 \times \exp\left(-\frac{\Delta G(\{n_i\}) - \Delta G(2,1,0)}{kT}\right), \tag{8}$$

where ρ_1 and ρ_2 are the number densities of free H_2O and H_2SO_4 molecules, respectively, and ρ_0 is the number density corresponding to the reference pressure 1 atm. The equilibrium constant for sulfuric acid dihydrate formation K_1K_2 is estimated, as explained in Ref. 16. The formation energy of a dihydrate according to the classical droplet model $\Delta G(2,1,0)$ is calculated from Eq. (1).

The H_2O–H_2SO_4 dihydrate is available as a reference point only for vapors containing both water and sulfuric acid, and thus the distribution of Eq. (8) cannot be used for other systems. For H_2O–HNO_3/MSA–NH_3 vapors we use the equilibrium distribution of Wilemski and Wyslouzil,[18]

$$\rho(\{n_i\}) = (p_{s,1})^{x_1}(p_{s,2})^{x_2}(p_{s,3})^{x_3} \times \exp(x_1\Theta_1 + x_2\Theta_2 + x_3\Theta_3) \times \left(\frac{p_1}{p_{s,1}}\right)^{n_1}\left(\frac{p_2}{p_{s,2}}\right)^{n_2}\left(\frac{p_3}{p_{s,3}}\right)^{n_3} \times \exp\left(\frac{-\sigma(\{n_i\})s(\{n_i\})}{kT}\right), \tag{9}$$

where $s(\{n_i\})$ is the surface area of the cluster and $\Theta_i = \sigma_i s_i(1)/(kT)$, where σ_i is the surface tension of pure liquid of type i and $s_i(1)$ is the surface area of monomer species i. Both Eqs. (8) and (9) obey the law of mass action and reduce to self-consistent classical unary or binary distributions at corresponding limits. The distribution used for H_2O–H_2SO_4–NH_3 vapors depends on the group of systems.

We assume that the derivatives in Eq. (7) are calculated with respect to core particle numbers n_{il} instead of total number of particles n_i. This approximation causes small errors in nucleation rates[7] but it speeds up and stabilizes the calculation considerably. The greatest errors are expected to occur in situations where n_{is} and n_{il} are of comparable magnitude; however, in these cases classical nucleation theory is not intrinsically very reliable.[13]

III. THERMODYNAMIC MODELS

The calculation of nucleation rates as described in the previous section requires an accurate knowledge of saturation vapor pressures, densities, and surface tensions of bulk substances over a wide range of temperatures and liquid compositions. These are obtained from thermodynamic models and parametrizations. In this study we have used almost

Downloaded 28 Nov 2002 to 128.214.57.32. Redistribution subject to AIP license or copyright, see http://ojps.aip.org/jcpo/jcpcr.jsp

exclusively thermodynamics readily available from published works on nucleation and chemical thermodynamics.

Equilibrium vapor pressures for $H_2O-H_2SO_4-NH_3$, $H_2O-H_2SO_4-HNO_3$, and $H_2O-HNO_3-NH_3$ systems are taken from the thermodynamic model of Clegg *et al.*[19] (http://www.hpc1.uea.ac.uk/~e770/aim.html). However, sulfuric acid vapor pressure is modified, as explained in our previous papers.[7,16] The calculation of surface tension and density of $H_2O-H_2SO_4-NH_3$ mixtures follows the method used in the more comprehensive study of this system.[7] Surface tension and density of $H_2O-H_2SO_4-HNO_3$ solutions are obtained from the parametrizations of Martin *et al.*[20] The density of the $H_2O-HNO_3-NH_3$ system is calculated according to the method of Van Dingenen and Raes.[11] For surface tension this method was modified to produce correct values at the $H_2O-NH_4NO_3$ limit. Surface tension of the $H_2O-NH_4NO_3$ solution is obtained from a fit to the data presented in the International Critical Tables.[21]

The equilibrium vapor pressures, density, and surface tension of $H_2O-HCl-NH_3$ solution are obtained from Arstila *et al.*[10] The thermodynamic treatment of $H_2O-H_2SO_4-MSA$ solution follows closely the work of Van Dingenen and Raes.[11] However, instead of treating H_2SO_4 as a 1:2 electrolyte, we calculate the actual HSO_4^- concentrations as described in the appendix of Ref. 11. We also modified the equilibrium constant for sulfuric acid to get the equilibrium vapor pressure of sulfuric acid close to that obtained from the model of Clegg *et al.*[19] Notwithstanding, the nucleation rates at the binary $H_2O-H_2SO_4$ limit are slightly different from those obtained from Clegg's model and, therefore, we have estimated the binary limit using a model appropriate to the system in question. We note that binary limits for all substances cannot be calculated due to the chemical characteristics of the solution or restrictions inherent to the model.

IV. RESULTS

A. $H_2O-H_2SO_4/HNO_3/HCl-NH_3$ vapors

The observed enhancement of nucleation when ammonia is added to $H_2O-H_2SO_4$ mixture is primarily due to the tendency of ammonia to decrease activity of sulfuric acid in the liquid phase above the solution surface. (Activity in the liquid phase is defined as $p_{s,i}/p_{\mathrm{pure},i}$, where $p_{\mathrm{pure},i}$ is the equilibrium vapor pressure of pure fluid i.) We can now ask whether this is also the case if sulfuric acid is replaced with another acid (HNO_3 or HCl). With this question in mind, we have plotted the liquid phase activity (or pressure in the case of HCl, for which pressure of the pure liquid cannot be obtained) of the acid as a function of ammonia molality.

Figure 1 shows our results for $H_2O-H_2SO_4-NH_3$ mixtures at $T=298.15$ K. Sulfuric acid molality is shown in the plot. It can be seen that H_2SO_4 activity decreases several orders of magnitude with increasing NH_3 molality unless H_2SO_4 molality is very small. Since the critical clusters in $H_2O-H_2SO_4-NH_3$ vapors are highly concentrated both in H_2SO_4 and NH_3,[7] the decrease in H_2SO_4 activity indeed seems to be related to nucleation behavior. Plots for $H_2O-HNO_3-NH_3$ and $H_2O-HCl-NH_3$ mixtures (Fig. 2) indicate similar trends but the overall decrease in acid activity

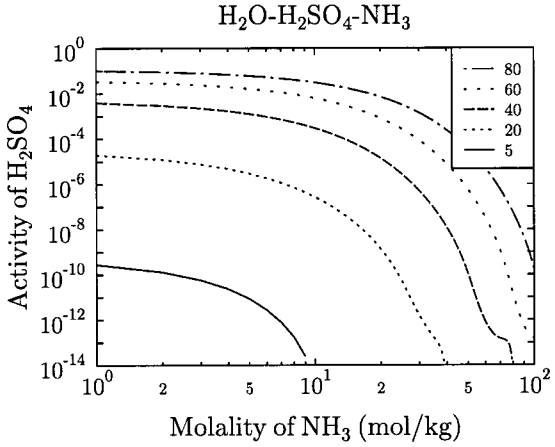

FIG. 1. Liquid phase activity of H_2SO_4 as a function of NH_3 molality. The molality of H_2SO_4 is shown in the legend. The temperature is 298.15 K.

(or pressure) is somewhat smaller. The curves end at binary $H_2O-NH_4NO_3$ [Fig. 2(a)] and H_2O-NH_4Cl [Fig. 2(b)] limits. Especially interesting is the behavior of HCl pressure, which shows an abrupt dip when NH_3 molality approaches to that of HCl. These results have an important consequence concerning nucleation. Although solutions with unequal amounts of NH_3 and HCl certainly exist, the mole fractions

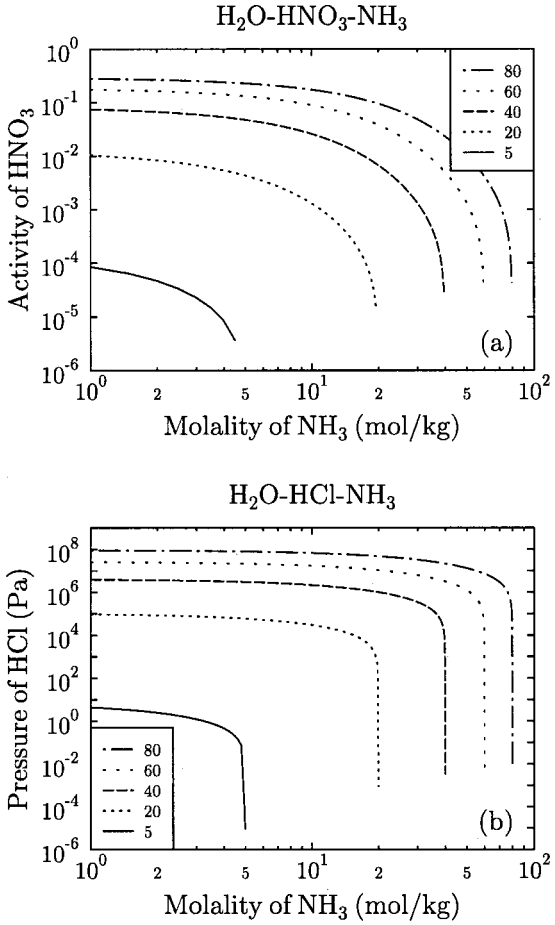

FIG. 2. Liquid phase activity of HNO_3 (a) and the pressure of HCl (b) above the solution surface as a function of the molality of NH_3. Molalities of HNO_3 and HCl are shown in the legends. The temperature is 298.15 K.

Downloaded 28 Nov 2002 to 128.214.57.32. Redistribution subject to AIP license or copyright, see http://ojps.aip.org/jcpo/jcpcr.jsp

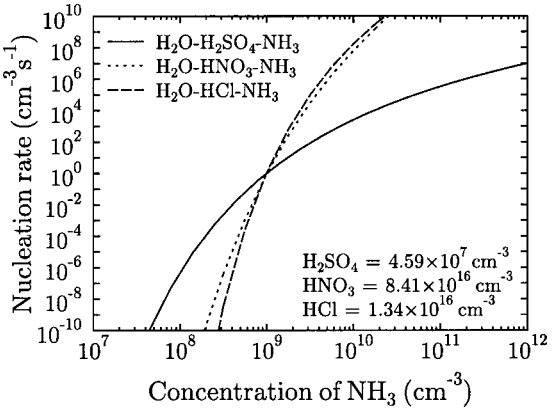

FIG. 3. The nucleation rate as function of NH_3 concentration. Concentrations of H_2SO_4, HNO_3, and HCl are shown in the figure. The temperature is 298.15 K and the relative humidity is 50%.

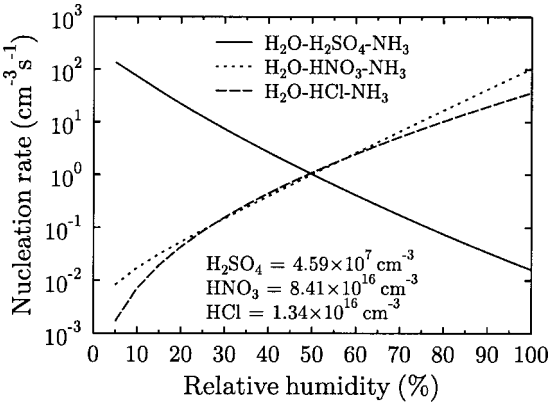

FIG. 4. Dependence of the nucleation rate on relative humidity for the systems containing NH_3. The concentration of the acid component is shown in the figure. The temperature is 298.15 K and the NH_3 concentration, 10^9 molecules/cm^3.

of HCl and NH_3 are always the same in the critical droplets because other compositions are energetically much more unfavorable.[10]

Figure 3 shows the dependence of nucleation rate on ammonia vapor concentration for the three systems at $T=298.15$ K and $RH=50\%$. The acid concentration is adjusted so that nucleation rate is 1 cm^{-3} s^{-1} when ammonia concentration is 10^9 molecules/cm^3. In this figure and for the rest of the paper, the H_2SO_4 concentration refers to the total concentration of H_2SO_4 (including H_2O–H_2SO_4 hydrates). Vapors containing nitric acid or HCl are most affected by ammonia. The nucleation rate increases over ten orders of magnitude if the ammonia concentration increases just one order of magnitude. Both these systems behave almost equally but the nucleation rate in H_2O–H_2SO_4–NH_3 vapors seems to depend less strongly on ammonia. This behavior can be related to the bulk properties presented in Figs. 1 and 2. The H_2O–H_2SO_4–NH_3 clusters are very concentrated in H_2SO_4 and NH_3, even at low nucleation rates, in Fig. 3. It then becomes obvious from Fig. 1 that adding more NH_3 in the vapor does not change equilibrium partial pressure (and presumably the nucleation rate) of H_2SO_4 very much. On the other hand, the critical clusters in H_2O–HNO_3–NH_3 and especially in H_2O–HCl–NH_3 vapors have a considerable amount of water at low nucleation rates. For these systems the drop in acid pressure is steepest at high NH_3 molalities, which explains the relatively strong effect of NH_3 on nucleation rates. As the nucleation rate approaches higher values, the slope of nucleation curves becomes less steep, owing to the same effect as in H_2O–H_2SO_4–NH_3 vapors.

The dependence of the nucleation rate on relative humidity at $T=298.15$ K is shown in Fig. 4. Ammonia concentration is 10^9 molecules/cm^3 and the acid concentration is adjusted to give the nucleation rate 1 cm^{-3} s^{-1} at $RH=50\%$. The nucleation rate in H_2O–HNO_3–NH_3 and H_2O–HCl–NH_3 systems increases as *RH* increases, but H_2O–H_2SO_4–NH_3 vapors exhibit opposite behavior. This phenomenon is caused by the depletion of free H_2SO_4 vapor molecules by hydration, as explained in Ref. 7.

A similar plot in Fig. 5 shows the temperature dependence of systems containing ammonia. We see here the same effect as in Fig. 3: because the H_2O–H_2SO_4–NH_3 clusters are practically water-free and there is little change in H_2SO_4 and NH_3 concentrations as a function of temperature, the dependence of the nucleation rate on temperature is rather modest. This is also the case for H_2O–HNO_3–NH_3 clusters at high nucleation rates. The mole fraction of water in H_2O–HCl–NH_3 clusters changes from 0.44 to 0.35 as the nucleation rate increases from $J=10^{-10}$ to $J=10^{10}$ cm^{-3} s^{-1}. Not surprisingly, the nucleation rate curve is steepest for these clusters.

Figure 6 depicts the ammonia and acid (H_2SO_4, HNO_3, or HCl) concentrations needed to obtain nucleation rate 1 cm^{-3} s^{-1} at 258.15 K and 298.15 K. The relative humidity is 50%. A mixture of H_2O, HCl, and NH_3 seems to nucleate somewhat better than H_2O–HNO_3–NH_3 in comparable conditions, although at low concentrations of NH_3 the situation is reversed. However, if H_2SO_4 is present instead of HNO_3 or HCl, the required acid concentrations are six to nine magnitudes lower. The strong temperature dependence of H_2O–HCl–NH_3 vapors is also apparent in this figure. The HCl concentrations are about four orders lower if the temperature is decreased from 298.15 to 258.15 K, the decrease

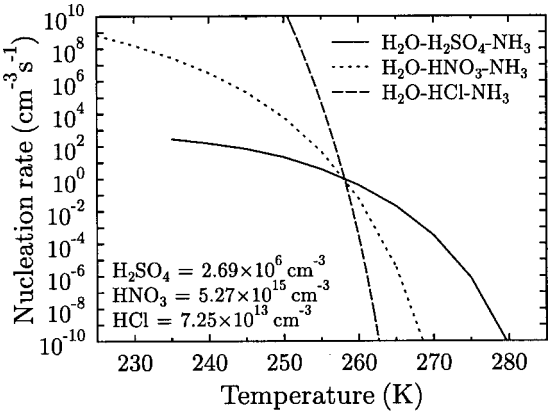

FIG. 5. Dependence of the nucleation rate on temperature for the systems containing NH_3. The concentration of NH_3 is 10^7 molecules/cm^3 and the concentrations of acids are shown in the figure. The relative humidity is 50%.

Downloaded 28 Nov 2002 to 128.214.57.32. Redistribution subject to AIP license or copyright, see http://ojps.aip.org/jcpo/jcpcr.jsp

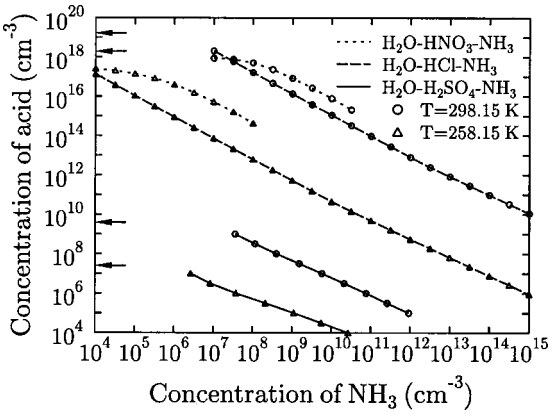

FIG. 6. Concentrations of NH_3 and acid (H_2SO_4, HNO_3, or HCl) corresponding to the nucleation rate $J=1\ \mathrm{cm}^{-3}\ \mathrm{s}^{-1}$ at temperatures 258.15 and 298.15 K. The relative humidity is 50%. The upper and lower pair of small arrows on the left indicate binary limits of H_2O–HCl and H_2O–H_2SO_4 nucleation, respectively. In each pair the lower arrow corresponds to temperature 258.15 and and the upper arrow to 298.15 K.

in acid concentration is three orders of magnitude or less in the case of H_2SO_4 or HNO_3. We also tested the effect of relative humidity on the required concentrations. Increasing the relative humidity to 90% lowers the curves of H_2O–HNO_3–NH_3 and H_2O–HCl–NH_3 systems but raises the curves of H_2O–H_2SO_4–NH_3 system, which is in accord with Fig. 4. However, the change in acid concentrations is less than one order of magnitude at a constant concentration of NH_3.

The small arrows on the left edge of Fig. 6 indicate binary H_2O–H_2SO_4 and H_2O–HCl limits at 258.15 and 298.15 K. Due to the problems associated with classical nucleation theory, we were not able to obtain reliable results for ammonia concentrations between the left ends of the H_2O–H_2SO_4–NH_3 curves and the limits of H_2O–H_2SO_4 nucleation.[7] Both of the curves of the H_2O–HNO_3–NH_3 system seem to bend toward a constant limit with decreasing NH_3 concentration, but numerical values at very low NH_3 concentrations proved inconclusive. Therefore the binary H_2O–HNO_3 limits are left out from Fig. 6. The binary nucleation rates for H_2O–HCl vapors were calculated from a computer program specially designed for this purpose, but the obtained values are still somewhat unreliable due to the problems in the kinetic prefactor of Eq. (6).

A set of quite interesting plots are shown in Fig. 7 that depicts the numbers of molecules corresponding to the curves of constant nucleation rate $J=1\ \mathrm{cm}^{-3}\ \mathrm{s}^{-1}$ of Fig. 6 at $T=298.15$ K. Clusters in H_2O–H_2SO_4–NH_3 vapors are mostly H_2SO_4 and NH_3, and water appears in the clusters only at low concentrations of ammonia. The same phenomenon is evident also in H_2O–HNO_3–NH_3 vapors, although the clusters have some water at all concentrations of NH_3, as shown in Fig. 7(b). The particle number curves of HNO_3 and NH_3 merge at a NH_3 concentration of approximately 3×10^{10} molecules/cm^3, corresponding to the H_2O–NH_4NO_3 limit.

The H_2O–HCl–NH_3 system can be considered as a H_2O–NH_4Cl mixture in the liquid state of droplets and, therefore, we have plotted the number of NH_4Cl molecules

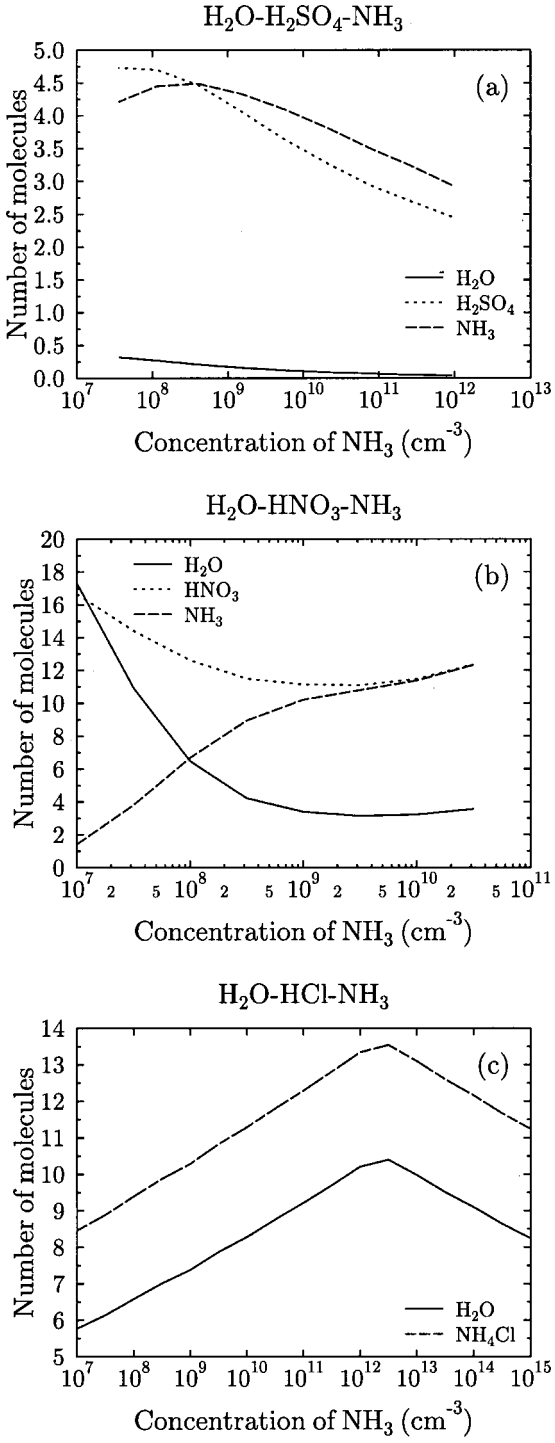

FIG. 7. The number of molecules in the critical nucleus corresponding to the curves of constant nucleation rate $J=1\ \mathrm{cm}^{-3}\ \mathrm{s}^{-1}$ at $T=298.15$ K in Fig. 6.

instead of numbers of HCl and NH_3 molecules separately. The particle number curves for this system in Fig. 7(c) show an intriguing maximum at a NH_3 concentration of about 3×10^{12} molecules/cm^3, with linear behavior elsewhere. This is a purely kinetic effect arising from the eigenvalue λ in Eq. (6), the absolute value of which shows a similar maximum at the same NH_3 concentration. In fact, if we plot curves of the constant formation energy of critical clusters ΔG^* instead of the constant nucleation rate, we find that the particle num-

Downloaded 28 Nov 2002 to 128.214.57.32. Redistribution subject to AIP license or copyright, see http://ojps.aip.org/jcpo/jcpcr.jsp

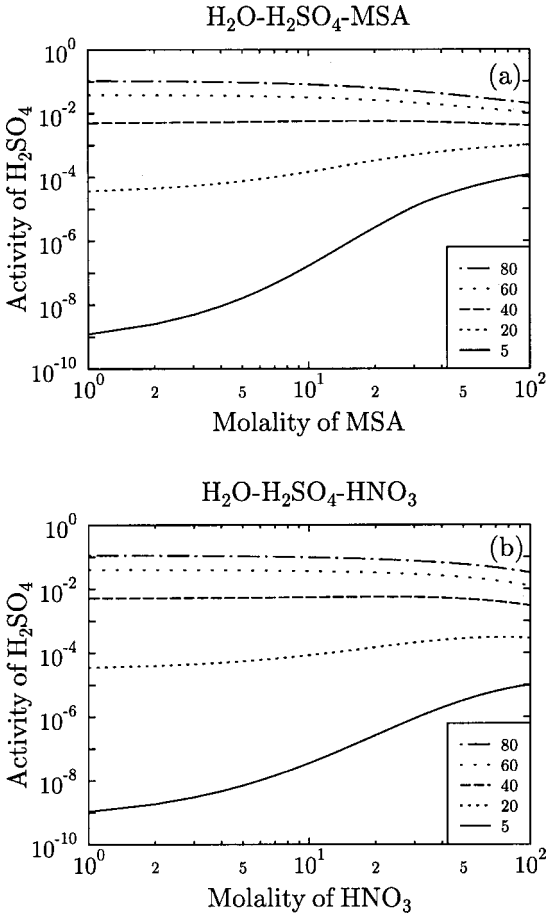

FIG. 8. The liquid phase activity of H_2SO_4 as a function of the molality of MSA (a) and HNO_3 (b). The molality of H_2SO_4 is shown in the legend. The temperature is 298.15 K.

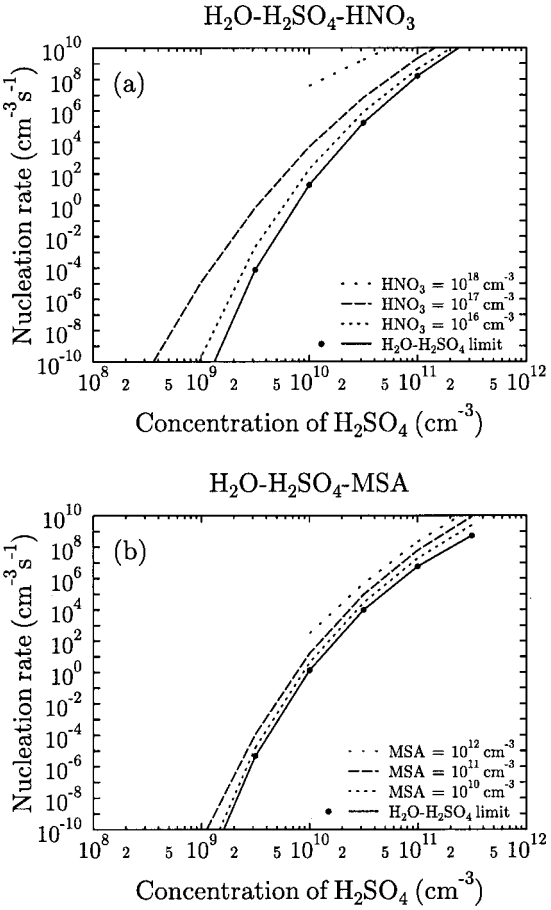

FIG. 9. The nucleation rate as a function of H_2SO_4 concentration for H_2O–H_2SO_4–HNO_3 (a) and H_2O–H_2SO_4–MSA (b) vapors. Concentrations of HNO_3 and MSA are indicated in the figure. A binary limit of H_2O–H_2SO_4 nucleation is shown as a solid line with filled circles. The relative humidity is 50%.

bers also stay constant. Close inspection reveals the nucleation rate curve of H_2O–HCl–NH_3 in Fig. 6 to be composed of two linear parts, with a downward cusp corresponding to the maximum in Fig. 7(c). At this point the vapor concentrations of NH_3 and HCl are equal, which makes it kinetically easier to form clusters because both molecular species are available in equal amounts for the formation of NH_4Cl. Hence, the required nucleation rate can be reached, even though the formation energy is higher and the cluster bigger than in vapors rich in NH_3 or HCl.

B. H_2O–H_2SO_4–NH_3/HNO_3/MSA vapors

Following the outline of the previous section, we begin the investigation of H_2O–H_2SO_4–HNO_3 and H_2O–H_2SO_4–MSA vapors by considering the effect of HNO_3 and MSA on the pressure of H_2SO_4 over bulk solutions. Figure 8 shows the liquid phase activity of H_2SO_4 as a function of MSA molality [Fig. 8(a)] and HNO_3 molality [Fig. 8(b)] at $T=298.15$ K. The behavior of acid activity is quite different from the that presented in Figs. 1 and 2. Adding MSA or HNO_3 to a H_2O–H_2SO_4 mixture decreases H_2SO_4 activity only a little at high H_2SO_4 molalities. In contrast, at low H_2SO_4 molalities the activity seems to increase. It is thus expected that MSA and HNO_3 do not facilitate the nucleation of H_2O–H_2SO_4 very much. Interestingly, the behavior of both the mixtures in Fig. 8 is almost identical.

We found that the calculation of nucleation rates for H_2O–H_2SO_4–HNO_3 and H_2O–H_2SO_4–MSA vapors was a much more difficult task than in the case vapors containing NH_3. We had to exclude clusters with a MSA or HNO_3 mole fraction more than about 0.1 from the results because in these cases the absolute value of the surface excess number of molecules for one acid component $|n_{i,s}|$ showed values comparable to $n_{i,l}$, often leading to negative number molecules n_i for this component. Similar difficulties arose when H_2SO_4 content increased in H_2O–HNO_3 or H_2O–MSA clusters. We attribute this behavior to the breakdown of classical nucleation theory already observed in H_2O–H_2SO_4–NH_3 vapors[7] and detailed elsewhere.[13,22] A likely explanation is that the surface of the clusters enriches with one acid component while the other resides in the cluster core. Despite the greatly reduced parameter space due to the above-mentioned difficulties, we were able to obtain suggestive results also for systems with two acid components.

Figure 9 illustrates the dependence of the nucleation rate on H_2SO_4 concentration for some MSA and HNO_3 concentrations. Also shown is the binary limit of H_2O–H_2SO_4

Downloaded 28 Nov 2002 to 128.214.57.32. Redistribution subject to AIP license or copyright, see http://ojps.aip.org/jcpo/jcpcr.jsp

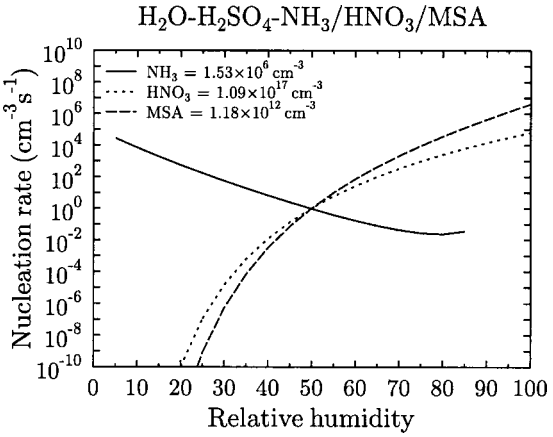

FIG. 10. Dependence of the nucleation rate on relative humidity for systems containing H_2SO_4. The temperature is 298.15 K and the H_2SO_4 concentration, 3.16×10^9 molecules/cm^3. Concentrations of acids are shown in the figure.

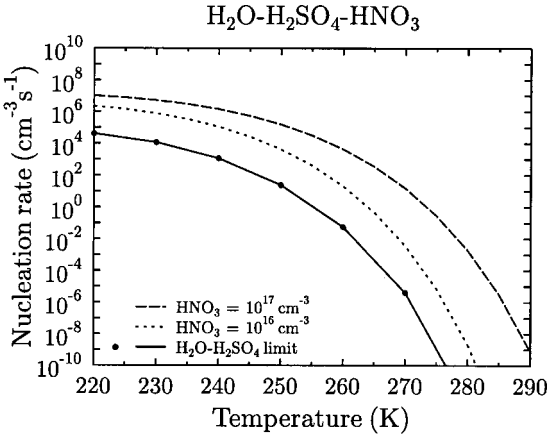

FIG. 11. Temperature dependence of the nucleation rate for H_2O–H_2SO_4–HNO_3 nucleation. Shown are lines for two HNO_3 concentrations and the binary H_2O–H_2SO_4 limit. The relative humidity is 50% and the concentration of H_2SO_4, 10^8 molecules/cm^3.

nucleation. Nitric acid seems to enhance nucleation significantly but the required HNO_3 concentrations are rather high. On the other hand, MSA affects the binary H_2O–H_2SO_4 nucleation very little. The unwillingness of two acids to form droplets is evident by the fact that the vapor concentrations of HNO_3 in Fig. 9(a) and MSA in parts of Fig. 9(b) are higher than the concentration of H_2SO_4, although the clusters are close to the H_2O–H_2SO_4 limit.

The dependence of the nucleation rate on relative humidity is shown in Fig. 10. Sulfuric acid concentration is 3.16×10^9 molecules/cm^3. The curves for H_2O–H_2SO_4–MSA and H_2O–H_2SO_4–HNO_3 systems show upward slopes, although hydration reduces the number of free H_2SO_4 molecules as *RH* increases. However, the observed behavior is consistent with the results obtained for a binary H_2O–H_2SO_4 system in similar conditions.[16] The curve for H_2O–H_2SO_4–NH_3, shown here for comparison, exhibits an altogether different trend. The nucleation rate first decreases with increasing *RH* and then reaches a minimum at *RH* $=80\%$ (values for relative humidities greater than 85% were omitted because the rapid increase in the water content of clusters caused similar problems with surface excess number of molecules, as mentioned earlier). The behavior of H_2O–H_2SO_4–NH_3 nucleation is probably related to the higher liquid mole fraction of H_2SO_4. Critical droplets of H_2O–H_2SO_4–HNO_3 and H_2O–H_2SO_4–MSA have a lower H_2SO_4 content and thus are less affected by the depletion of free H_2SO_4 vapor molecules.

The thermodynamic model of the H_2O–H_2SO_4–MSA system is restricted to temperature $T=298.15$ K. Therefore, we present a temperature dependence of the nucleation rate only for H_2O–H_2SO_4–HNO_3 vapors, together with the H_2O–H_2SO_4 limit. As shown in Fig. 11, the temperature dependence of H_2O–H_2SO_4–HNO_3 nucleation exhibits similar nearly constant behavior at low temperatures as the H_2O–H_2SO_4–NH_3 system.[7] This is particularly interesting because the clusters at 220 K are water rich as opposed to the clusters in H_2O–H_2SO_4–NH_3 vapors. By analogy with the H_2O–H_2SO_4–NH_3 system, one would expect a diminishing water content in the critical clusters with decreasing temperature and a stronger effect on the nucleation rate, but, obviously, the conucleation of H_2SO_4 and HNO_3 is not energetically favorable.

Finally, we present a comparison of nucleation rates as a function of the third component (NH_3, HNO_3, or MSA). Figure 12 illustrates nucleation rates corresponding to H_2SO_4 concentration of 10^7 molecules/cm^{-3} and relative humidity 90%. The HNO_3 concentration needed to reach e.g., the nucleation rate $J=1$ cm^{-3} s^{-1} is six orders of magnitude higher than the required NH_3 concentration. Concentrations of NH_3 and MSA are closer together and, at very high nucleation rates, the curves of H_2O–H_2SO_4–NH_3 and H_2O–H_2SO_4–MSA even seem to intersect. It should be noted that the curve for H_2O–H_2SO_4–MSA system is close to the binary H_2O–MSA limit. The nucleation rate at the binary H_2O–H_2SO_4 limit at the conditions of this plot is about 10^{-52} cm^{-3} s^{-1}.

V. DISCUSSION AND CONCLUSIONS

In this paper we have compared various ternary nucleation routes involving water, sulfuric acid, nitric acid, hydrochloric acid, methane sulfonic acid, and ammonia. The sys-

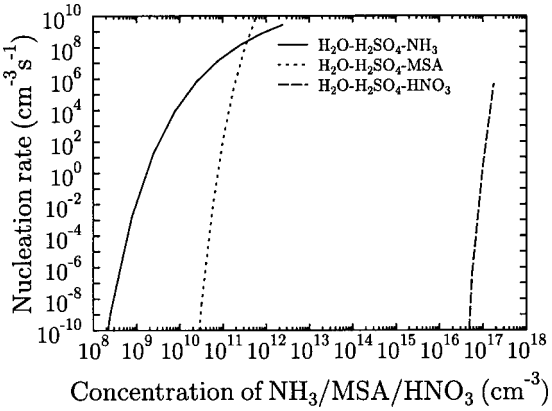

FIG. 12. The nucleation rate as a function of NH_3, MSA, or HNO_3 concentration for the systems containing H_2SO_4. The concentration of H_2SO_4 is 10^7 molecules/cm^3 and the relative humidity is 90%.

Downloaded 28 Nov 2002 to 128.214.57.32. Redistribution subject to AIP license or copyright, see http://ojps.aip.org/jcpo/jcpcr.jsp

tems are treated in a theoretically consistent manner using classical nucleation theory and existing thermodynamic models. The results show that ammonia helps the nucleation of water–acid vapors. However, the relative order of importance of different ternary nucleation mechanisms in comparable acid concentrations is primarily determined by the binary water–acid limits; to achieve similar nucleation rates in $H_2O–HNO_3–NH_3$ or $H_2O–HCl–NH_3$ vapors as in $H_2O–H_2SO_4–NH_3$ vapors requires extremely high concentrations of NH_3.

The presence of HNO_3 or MSA in $H_2O–H_2SO_4$ vapors appears to have little effect on nucleation rates. However, we were not able to investigate all combinations of parameters due to the instability of the nucleation model and the limitation of the thermodynamical model to one temperature in the case of MSA. It, nevertheless, seems that high concentrations of HNO_3 or MSA are needed to produce results that are significantly divergent from the binary $H_2O–H_2SO_4$ limit. Intriguingly though, if similar NH_3 and MSA concentrations are compared, the binary H_2O–MSA nucleation rate may even exceed the ternary $H_2O–H_2SO_4–NH_3$ nucleation rate in some occasions. It is worth mentioning that our results for $H_2O–H_2SO_4$–MSA vapors are not consistent with those of Van Dingenen and Raes.[11] This is probably due to the differences in the treatment of H_2SO_4 dissociation.

A comprehensive assessment of ternary nucleation in various ambient conditions often requires lengthy calculations. We found that by just monitoring the effect a third chemical component on the acid pressure above a bulk solution yields qualitative information how the nucleation behavior changes relative to the binary water–acid system. We by no means suggest this as a generally valid method because the characteristics of nucleation depend on vapor pressures of all the substances and, in addition, on surface tension. Moreover, any deductions assume some knowledge of mole fractions in the cluster. It is also important to bear in mind that nucleation rate is not related to the formation energy of the critical nucleus in a simple manner. The kinetic part may have a significant effect on nucleation rate depending on the ambient vapor concentrations, as we illustrated in the case of $H_2O–HCl–NH_3$ vapors.

The reliability of our calculations is restricted by the well-known shortcomings of classical nucleation theory. In particular, the classical theory relies on the capillarity approximation, which states that surface tension is independent of the curvature of the droplet surface. While this assumption certainly skews the results, it may be totally invalid for clusters containing only a couple of molecules. In Fig. 7 we saw that $H_2O–HNO_3–NH_3$ and $H_2O–HCl–NH_3$ clusters contain approximately 30 molecules at 298.15 K, whereas $H_2O–H_2SO_4–NH_3$ clusters have only five to ten molecules. At 258.15 K the $H_2O–HCl–NH_3$ droplets are of the same size as at the higher temperature but the clusters sizes of the other two systems are diminished by half. A similar comparison can be made based on Fig. 12 where nucleation rates in vapors containing both water and sulfuric acid are presented. At nucleation rate 1 $cm^{-3}s^{-1}$ the droplets in systems with NH_3, MSA, and HNO_3 consist of about 13, 60, and 90 molecules, respectively. For all the systems studied in this paper, the molecular content of droplets decreases approximately by half if nucleation rate increases from 1 to 10^6 $cm^{-3}s^{-1}$. On the grounds of these considerations it seems that the nucleation calculations are most unreliable for the $H_2O–H_2SO_4–NH_3$ system. However, we believe that this should not affect the general conclusions, because the same relative importance of different nucleation routes can also be found at lower nucleation rates ($\ll 1$ $cm^{-3}s^{-1}$), where $H_2O–H_2SO_4–NH_3$ clusters are considerably bigger.

The results of this study have profound implications regarding nucleation in atmospheric conditions. The concentrations of HNO_3 or HCl required to reach significant nucleation rates in presence of ammonia are far higher than measured in the atmosphere.[23] Also, it is hardly conceivable that enough ammonia could be found to make $H_2O–HNO_3–NH_3$ or $H_2O–HCl–NH_3$ important nucleation routes in the atmosphere. Nucleation of $H_2O–H_2SO_4–HNO_3$ is not likely to occur in atmospheric conditions either. Lastly, the effect of MSA to $H_2O–H_2SO_4$ nucleation seems rather meager. Not counting other mechanisms of particle production or nucleation enhancement, the results of this study strongly endorses $H_2O–H_2SO_4–NH_3$ nucleation over other studied ternary nucleation pathways as the most likely route of new particle formation in the atmosphere. Investigations of other possible combinations of substances and nucleation involving four chemical components are left for future study.

ACKNOWLEDGMENT

This work was supported by the Academy of Finland (Project No. 47668).

[1] C. O'Dowd *et al.*, Geophys. Res. Lett. **26**, 1707 (1999).
[2] R. J. Weber *et al.*, Geophys. Res. Lett. **26**, 307 (1999).
[3] W. Birmili, A. Wiedensohler, C. Plass-Dülmer, and H. Berresheim, Geophys. Res. Lett. **27**, 2205 (2000).
[4] R. Harrison *et al.*, J. Geophys. Res. **105**, 17819 (2000).
[5] M. Kulmala *et al.*, Tellus, Ser. B **53**, 324 (2001).
[6] P. Korhonen *et al.*, J. Geophys. Res. **104**, 26349 (1999).
[7] I. Napari, M. Noppel, H. Vehkamäki, and M. Kulmala, J. Chem. Phys. **116**, 4221 (2002).
[8] R. C. Easter and R. K. Peters, J. Appl. Meteorol. **33**, 775 (1994).
[9] E. Nilsson and M. Kulmala, J. Geophys. Res. **103**, 1381 (1998).
[10] H. Arstila, P. Korhonen, and M. Kulmala, J. Aerosol Sci. **30**, 131 (1999).
[11] R. Van Dingenen and F. Raes, J. Aerosol Sci. **24**, 1 (1993).
[12] W. D. Scott and F. C. R. Cattell, Atmos. Environ. **13**, 307 (1979).
[13] A. Laaksonen, R. McGraw, and H. Vehkamäki, J. Chem. Phys. **111**, 2019 (1999).
[14] H. Trinkaus, Phys. Rev. B **27**, 7372 (1983).
[15] K. Binder and D. Stauffer, Adv. Phys. **25**, 343 (1976).
[16] M. Noppel, H. Vehkamäki, and M. Kulmala, J. Chem. Phys. **116**, 218 (2002).
[17] M. Noppel, in *Nucleation and Atmospheric Aerosols 2000*, 15th International Conference, edited by B. Hale and M. Kulmala (AIP Conf. Proc., Melville, NY, 2000), Vol. 534, pp. 339–342.
[18] G. Wilemski and B. E. Wyslouzil, J. Chem. Phys. **103**, 1127 (1995).
[19] S. L. Clegg, P. Brimblecombe, and A. S. Wexler, J. Phys. Chem. A **102**, 2137 (1998).
[20] E. Martin, C. George, and P. Mirabel, Geophys. Res. Lett. **27**, 197 (2000).
[21] *International Critical Tables of Numerical Data Physics, Chemistry and Technology* (McGraw-Hill, New York, 1928), Vol. I, pp. 56–57.
[22] A. Laaksonen and I. Napari, J. Phys. Chem. B **105**, 11678 (2001).
[23] M. Kulmala, A. Toivonen, T. Mattila, and P. Korhonen, J. Geophys. Res. **103**, 16183 (1998).

Downloaded 28 Nov 2002 to 128.214.57.32. Redistribution subject to AIP license or copyright, see http://ojps.aip.org/jcpo/jcpcr.jsp